

November 7, 1967

VSH-M-1782

Dear Joe:

Subject:

STATINTL

In accordance with Contract requirements, enclosed is one copy of
Engineering Report 8959, Refinement of Techniques, Final Report,

Regards,

Gus

STATINTL

vsh
cc:
Attachments

Declass Review by NIMA/DOD

STATINTL

Approved For Release 2002/06/17 : CIA-RDP78B04747A000700010024-8

Approved For Release 2002/06/17 : CIA-RDP78B04747A000700010024-8

STATINTL



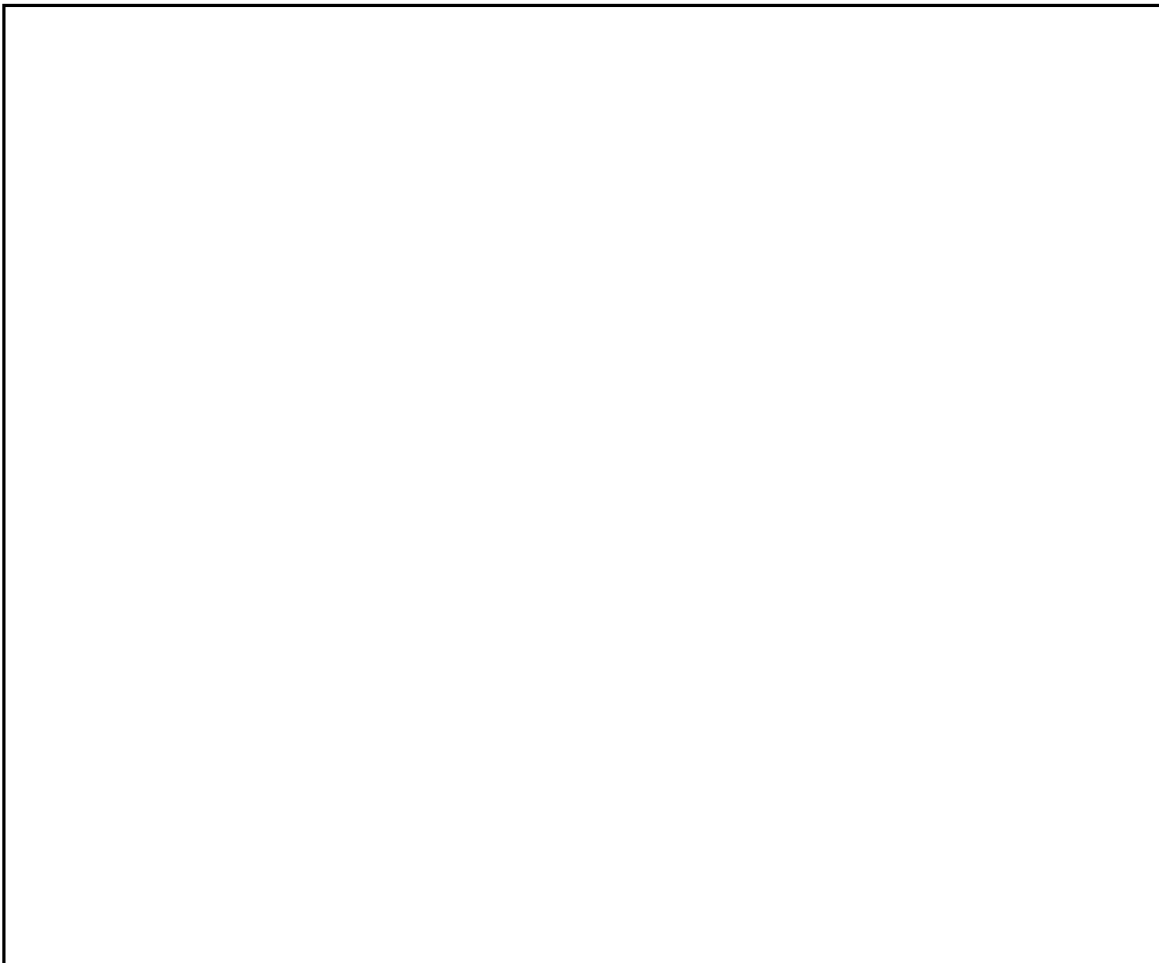
ENGINEERING REPORT NO. 8959

REFINEMENT OF TECHNIQUES

FINAL REPORT

DATE: 3 October 1967

STATINTL



Contributor:

TABLE OF CONTENTS

<u>Section</u>	<u>Title</u>	<u>Page</u>
	Abstract	iii
I	TECHNIQUES INVESTIGATED	1
	1.1 Introduction	1
	1.2 Simulation Aspects	1
	1.3 Instrumentation Aspects	2
II	SIMULATION AND INSTRUMENTATION STUDIES	3
	2.1 Printer MTF Control	3
	2.2 Pseudo GEMS Viewer MTF Control	15
	2.3 Exposure Simulation Control	24
	2.4 Haze Simulation Control	25
	2.5 Equipment Modifications and Improvements	38
III	STUDY TASK CONCLUSIONS	40
	3.1 Simulation Summary Conclusions	40
	3.2 Instrumentation Summary Conclusions	41
	REFERENCES	43

LIST OF ILLUSTRATIONS

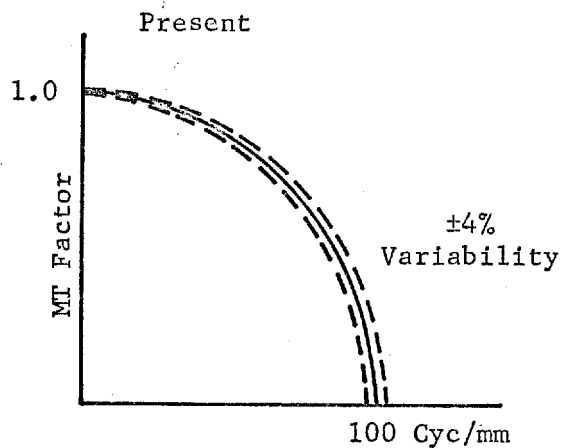
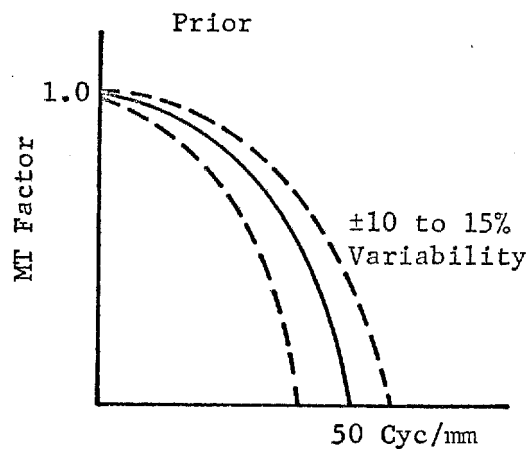
<u>Figure</u>	<u>Title</u>	<u>Page</u>
1	Simulation Geometry	4
2	Near-Field Effect Case A ($K_M = 50$ cy./mm.)	9
3	Near-Field Effect Case B ($K_M = 100$ cy./mm.)	10
4	Near-Field Effect Case C ($K_M = 150$ cy./mm.)	11
5	Near-Field Effect Case D ($K_M = 200$ cy./mm.)	12
6	Near-Field Effect Case E ($K_M = 250$ cy./mm.)	13
7	Near-Field Effect Case F ($K_M = 300$ cy./mm.)	14
8	Gamma 2.3 Characteristic Curve	17
9	Resulting EGA Curves	19
10	160 cyc/mm Simulation	21
11	120 cyc/mm Simulation	22
12	80 cyc/mm Simulation	23
13	Determination of Effective Exposure	27
14	Tone Reproduction Analysis of Atmospheric Haze	36

<u>Table</u>	<u>Title</u>	<u>Page</u>
1	GEMS Parameters	8
2	Predicted vs. Measured Exposure Modulation Values	35

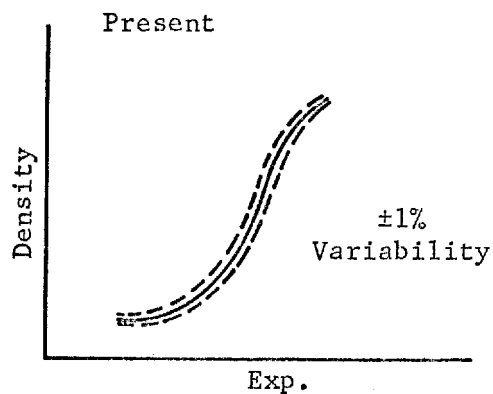
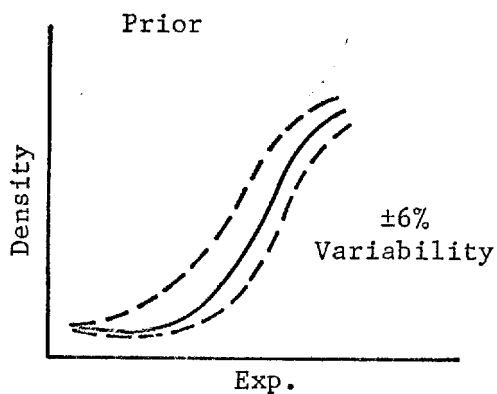
ABSTRACT

The Refinement of Techniques task was concerned with improving the GEMS simulation techniques and determining the accuracy of the simulation instrumentation. As illustrated in Figure 1, large magnitude refinements have been made in the control of the simulations. This degree of control provides the capability of generating fine matrix increment elements of each system parameter.

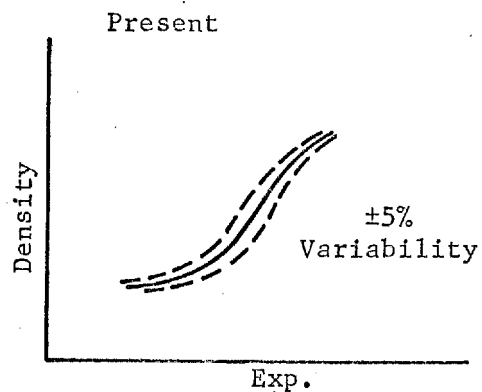
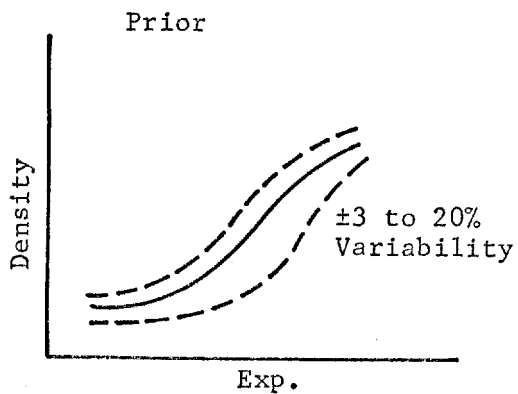
A. MTF Control



B. Exposure Control



C. Contrast Control*



*Potential control capability of ±1% variability with modification of instrumentation.

Figure 1. Accuracy of Simulation Instrumentation
(Modified Contact Printer)

SECTION I

TECHNIQUES INVESTIGATED

1.1 INTRODUCTION

The Refinement of Techniques task was established primarily for investigating and improving the simulation techniques and instrumentation. The specific areas investigated were:

- (a) Modulation transfer function (MTF) simulation on the modified contact printer
- (b) MTF simulation in the Pseudo GEMS Viewer
- (c) Exposure simulation
- (d) Haze simulation
- (e) Equipment modifications

Other study areas included under this task were the Gamma 2.3 Sensitometric study, the Equal Magnification GEMS study, and the System Parameters study. Separate final reports have been submitted for each of the above three studies.

1.2 SIMULATION ASPECTS

In the simulation of MTF by means of a modified contact printer, the investigation was concerned with the accuracy of control of the MTF at spatial frequencies above 100 cycles per millimeter. A second area of MTF simulation involved the use of a gamma 2.3 negative transparency in the Pseudo GEMS Viewer. An analytical study was performed to determine the degree of error introduced in simulating the MTF when employing non-linear film imagery in the viewer.

The simulation processes of exposure and haze were investigated to determine the accuracy of the techniques and the realism of the resulting imagery.

1.3 INSTRUMENTATION ASPECTS

The GEMS modified contact printer instrumentation was improved for more accurate control of the simulation processes. A new light source was installed to allow very short exposure times. The base plate of the printer was modified with a vacuum platen and jiggling to permit accurate control of the master transparency - unexposed film separation.

An aerial image sensitometric read-out device was breadboarded for use in copy camera systems. The device is used to acquire accurate sensitometric exposure data for edge gradient analysis (EGA) purposes.

SECTION II

SIMULATION AND INSTRUMENTATION STUDIES

2.1 PRINTER MTF CONTROL

The theory for controlling the simulation of MTF on a GEMS modified contact printer has been presented in a number of study reports. The discussion to follow assumes that the reader is familiar with the theory. When initially commencing the second GEMS Study program, a question was raised as to the validity of the simulated MTF at spatial frequencies above 100 cycles per millimeter. Rough order approximations indicate that uncontrolled degradations due to near-field diffraction may become significant at this spatial frequency level. Therefore, an investigation into such effects was conducted.

2.1.1 Analysis

The method used in the simulation process to produce a scene with a specified MTF is shown in Figure 1. A suitable mask is illuminated with incoherent light; the mask acts as the illumination source in the printer system. The master transparency and film are separated by a glass spacer. An exposure of the transparency scene is made on the film. The resultant spread function of the exposure will be:

$$S_E(x) = S_S\left(x/m_1\right) * S_T\left(x/m_2\right) * S_F(x)$$

The MTF of the exposure will be given by:

$$M_E(k) = M_S(m_1.k) \cdot M_T(m_2.k) \cdot M_F(k)$$

$$\text{with } m_1 = \frac{v}{u} \text{ and } m_2 = \frac{u+v}{u}$$

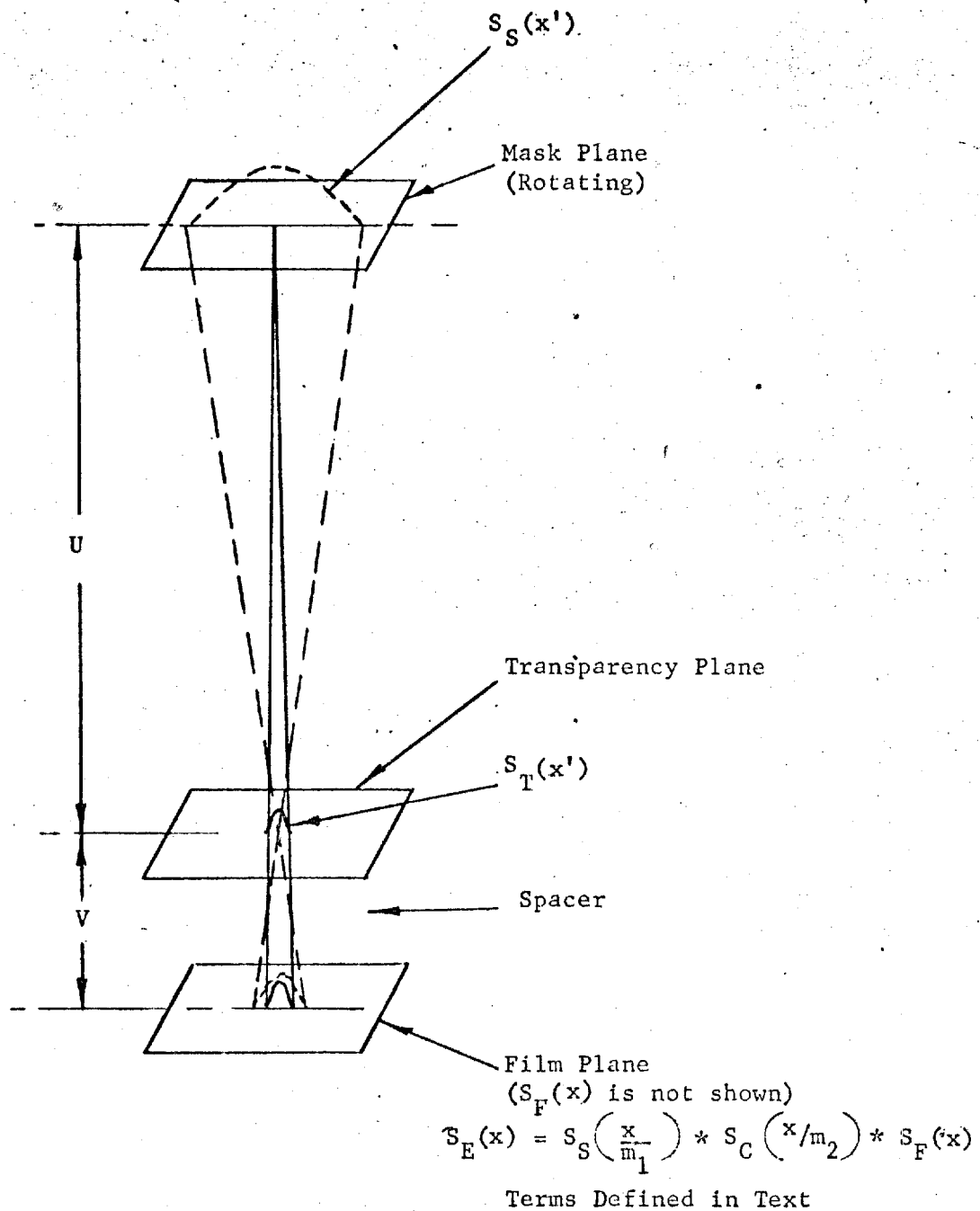


Figure 1. Simulation Geometry

where - x is the distance in the film plane,

k is the spatial frequency of interest in the film plane,

u is the distance between the source plane and the transparency plane,

v is the distance between the transparency plane and the film plane ($v \ll u$),

$S_S(x')$ and $M_S(k')$ are the spread function and the MTF (Fourier transform of the spread function) of the mask in the source plane,

$S_T(x')$ and $M_T(k')$ are the spread function and the MTF of the transparency in the transparency plane,

$S_F(x)$ and $M_F(k)$ are the spread function and the MTF of the film used in the exposure, and $*$ represents the convolution operation.

The use of the factors m_1 and m_2 translate the values of the MTF's from their original planes to the plane of the film. This procedure allows the production of the desired MTF for the final exposure. However, the condition for near-field (or Fresnel) diffraction exists, since the transparency and the film plane are separated by a finite distance. At high spatial frequencies, this degrading factor may become significant; it is necessary to investigate the effects of near-field diffraction upon the photographic simulation procedure.

In order to simplify the examination of the near-field effects, the initial assumption of a point source and a knife-edge object are made. The extension to mask shapes of finite size and imperfect edge objects can then be made. The expression for the intensity due to near-field diffraction of a knife-edge is given by:

$$I(x) = \frac{I_0}{2} \left\{ \left[\operatorname{sgn}(x) C(bx) - .5 \right]^2 + \left[\operatorname{sgn}(x) S(bx) - .5 \right]^2 \right\}$$

where - x is the distance in the film plane measured perpendicularly to the edge from the geometrical center.

I_0 is the intensity for the image plane if no knife-edge was present,

$\text{sgn}(x)$ is +1 when x is positive and is -1 when x is negative.

$$b = \sqrt{2/v\lambda},$$

λ is the wavelength of the illumination,

$C(bx)$ and $S(bx)$ are the Fresnel integrals given by:

$$C(bx) = \int_0^{bx} \cos \frac{\pi (z)^2}{2} dz$$

$$S(bx) = \int_0^{bx} \sin \frac{\pi (z)^2}{2} dz$$

The intensity change due to the extended source can be added by integration over the resulting spread function in the film plane.

$$I'(x) = \int_{-\infty}^{\infty} I(x-y) S(y) dy$$

where - $S(y)$ is the spread function of the mask in the film plane,

and

y is a distance in the film plane measured perpendicular to the edge from the geometrical center.

Actually, this equation is seen to be the convolution of two functions. If desired, $S(y)$ also could contain the effects of the transparency MTF and film MTF; then, $I'(X)$ would be an edge representative of all printer system degradation. If near-field effects were not present, the Fourier transform of $\frac{dI'(x)}{dx}$ would then represent the final MTF of the exposure. Actually, the case of most interest is given by a Gaussian spread function:

$$S(y) = e^{-y^2/2s^2} \quad \text{which is truncated after a finite distance,}$$

Y_f , where

$s = \frac{\sigma v}{u}$, and σ is a parameter of the spread function in the mask plane. The complete expression for $I'(X)$ is quite complex:

$$I'(X) = \frac{I_0}{2} \int_{-Y_f}^{Y_f} e^{-u^2 y^2 / 2 \sigma^2 v^2} \left\{ \left[\operatorname{sgn}(x-y) \int_0^b (x-y) \cos \frac{\pi z^2}{2} dz - .5 \right]^2 + \left[\operatorname{sgn}(x-y) \int_0^b (x-y) \sin \frac{\pi z^2}{2} dz - .5 \right]^2 \right\} dy$$

A computer program was developed for providing information on an intensity distribution as represented by the above equation for $I'(X)$ with any desired parameters of the printer system. It provides the edge shape for the geometrical case - exclusive of near-field effects, for the near-field case-exclusive of geometrical effects, and for the geometrical near-field combination. The output includes the parameter values: u , v , σ , and λ . The procedure also allows for integration over the spectral sensitivity response range when use of a single wavelength is not suitable. Tapes were produced of edge exposure values. These tapes were used with the edge-gradient analysis computer program to determine the printer system MTF. However, these MTF determinations are only valid for edges which are unaltered or only slightly altered by near-field diffraction, since complete data was not computed for more seriously degraded edges.

STATINTL

2.1.2 Results and Conclusions of Analysis

The computer program was used to provide test results for certain printer system specifications. Preliminary test results indicated the best choice of parameters to minimize near-field effects. The value of $m_1 = \frac{v}{u}$ is determined by the desired MTF cut-off spatial frequency (k_m) for the exposure. To achieve best results, the value v should be minimized; this also means minimizing u , since $u = v/m_1$. For high spatial frequency MTFs, the limit is

reached when u reaches the smallest distance possible for the geometry. The parameter σ should be large enough to permit reasonable distances; its size is also limited due to illumination conditions. It was definitely apparent that near-field degradation becomes a more serious problem at higher spatial frequencies.

An additional series of tests was directed towards determining near-field effects for optimum conditions with the present geometry. The spatial frequency range from 50 to 300 cycles per millimeters was examined. The graphs for these six cases are shown in Figures 2 through 7. The value for the parameters used are given in Table I.

TABLE I - GEMS PARAMETERS

<u>Case</u>	<u>k_m (cycles/mm.)</u>	<u>u (inches)</u>	<u>v (inches)</u>	<u>σ (inches)</u>	<u>λ (microns)</u>
A	50	12.	.0144	.328	.65
B	100	12.	.0072	.328	.65
C	150	12.	.0048	.328	.65
D	200	16.	.0048	.328	.65
E	250	20.	.0048	.328	.65
F	300	24.	.0048	.328	.65

The cut-off spatial frequency, k_m , is obtained from $s \cdot k_m = 1/2$, or $k_m = u/2\sigma v$. For this value, the expected modulation factor is approximately .007. The values $u = 12$ inches and $v = .0048$ inches are approximately minima for the system. The value of $\sigma = .328$ inches is the parameter for a Gaussian mask presently in use and is close to a maximum value.

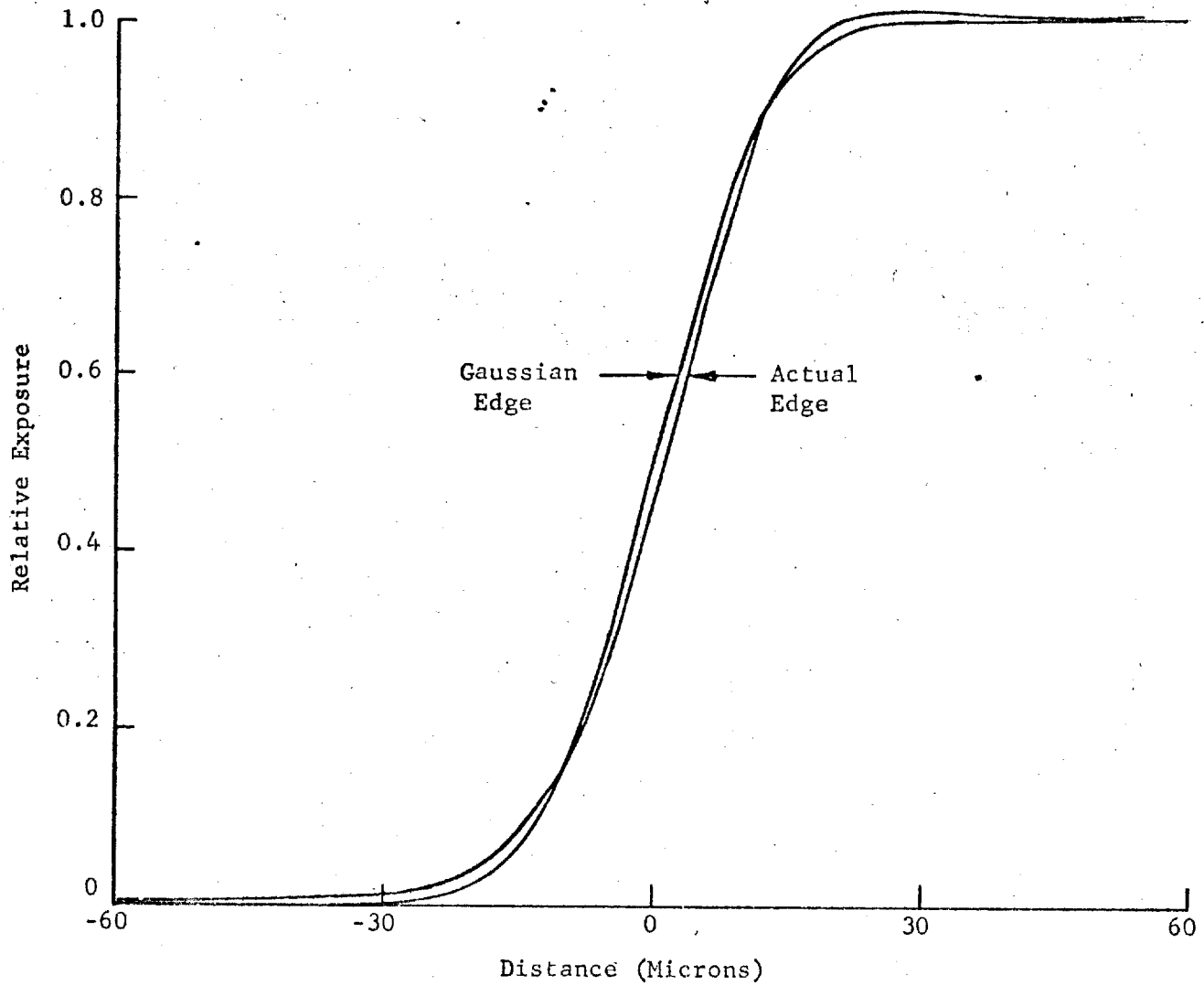


Figure 2. Near-Field Effect
Case A ($K_M = 50$ cy./mm.)

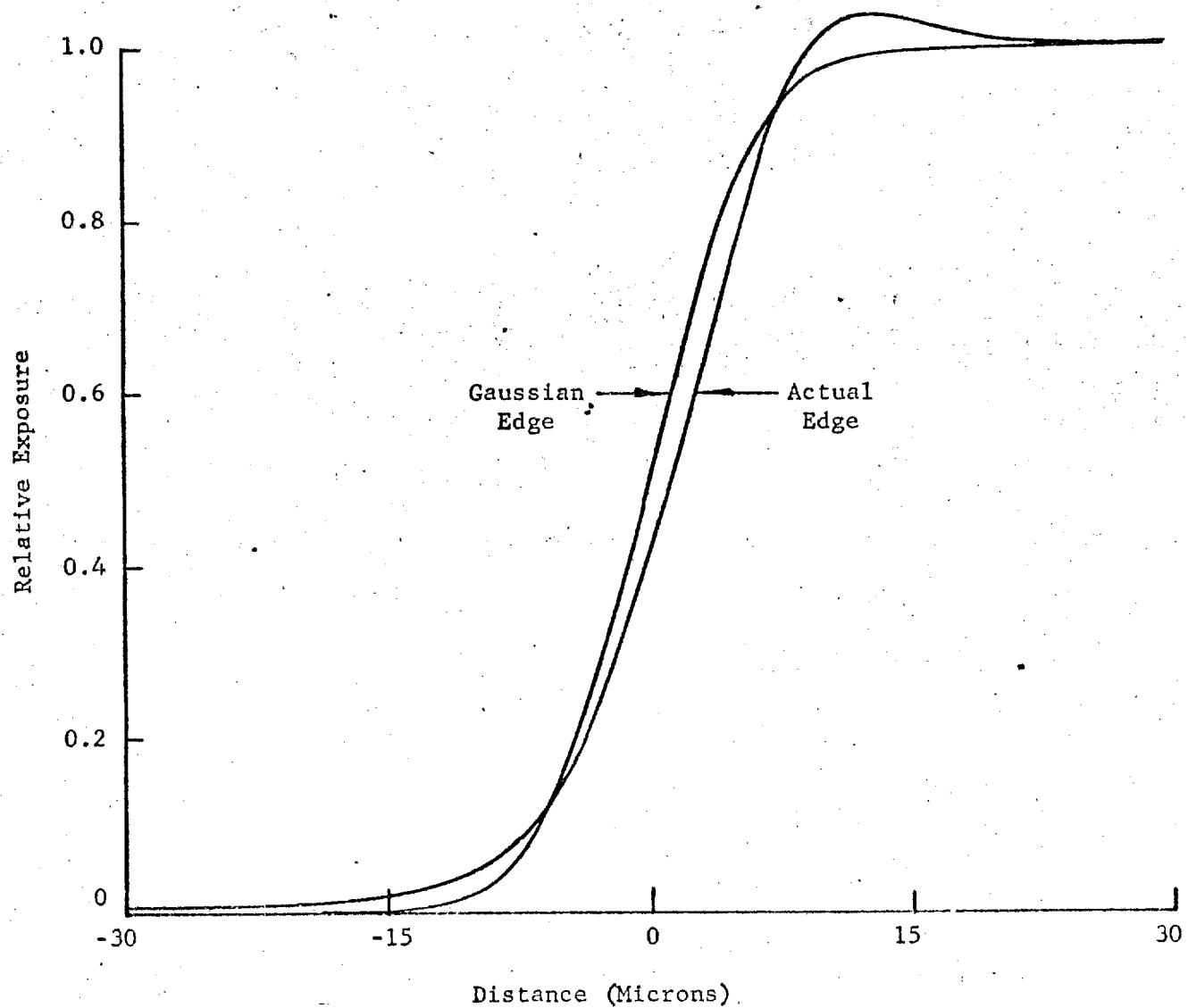


Figure 3. Near-Field Effect
Case B ($K_M = 100$ cy./mm.)

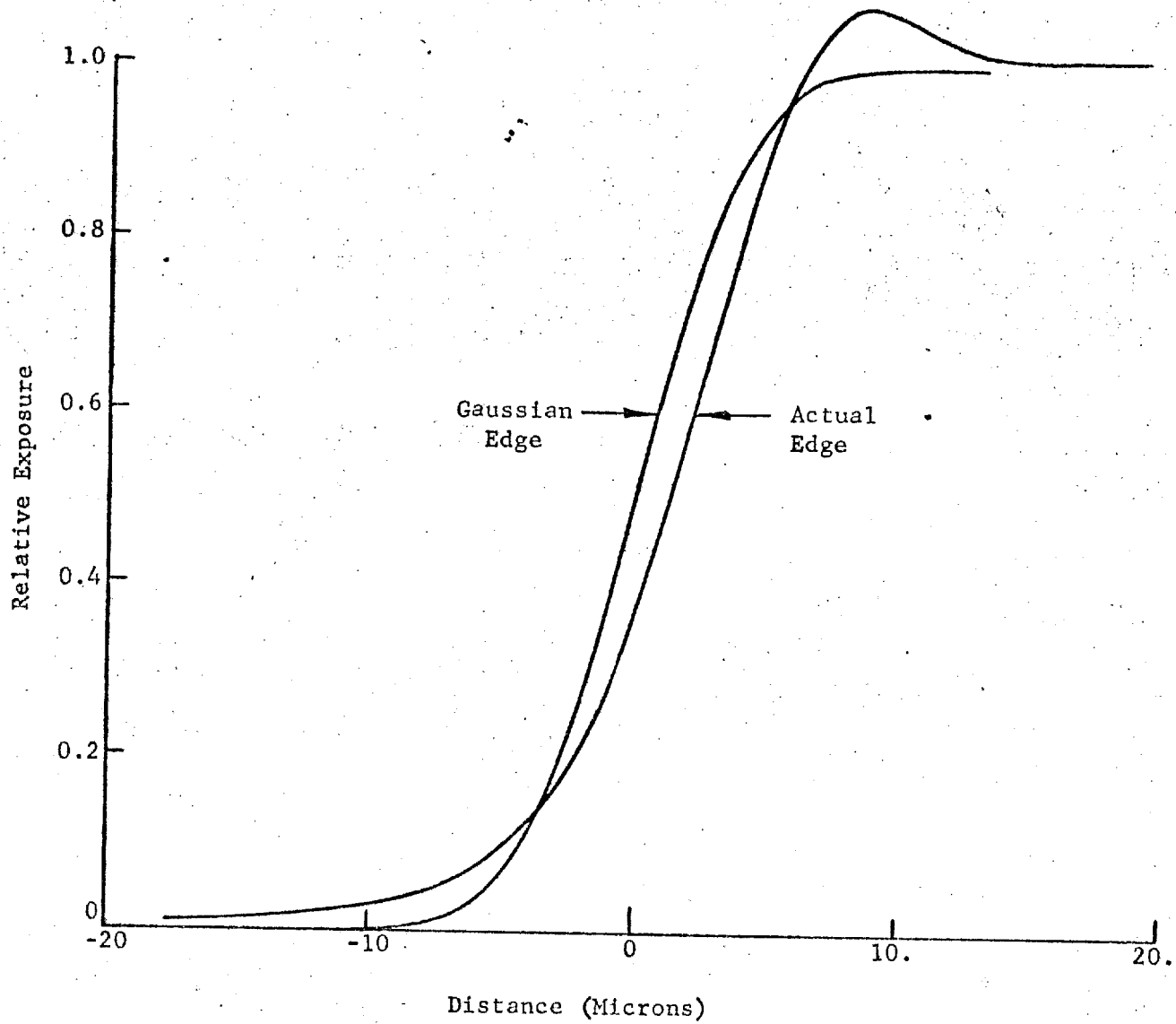


Figure 4. Near-Field Effect
Case C ($K_M = 150$ cy./mm.)

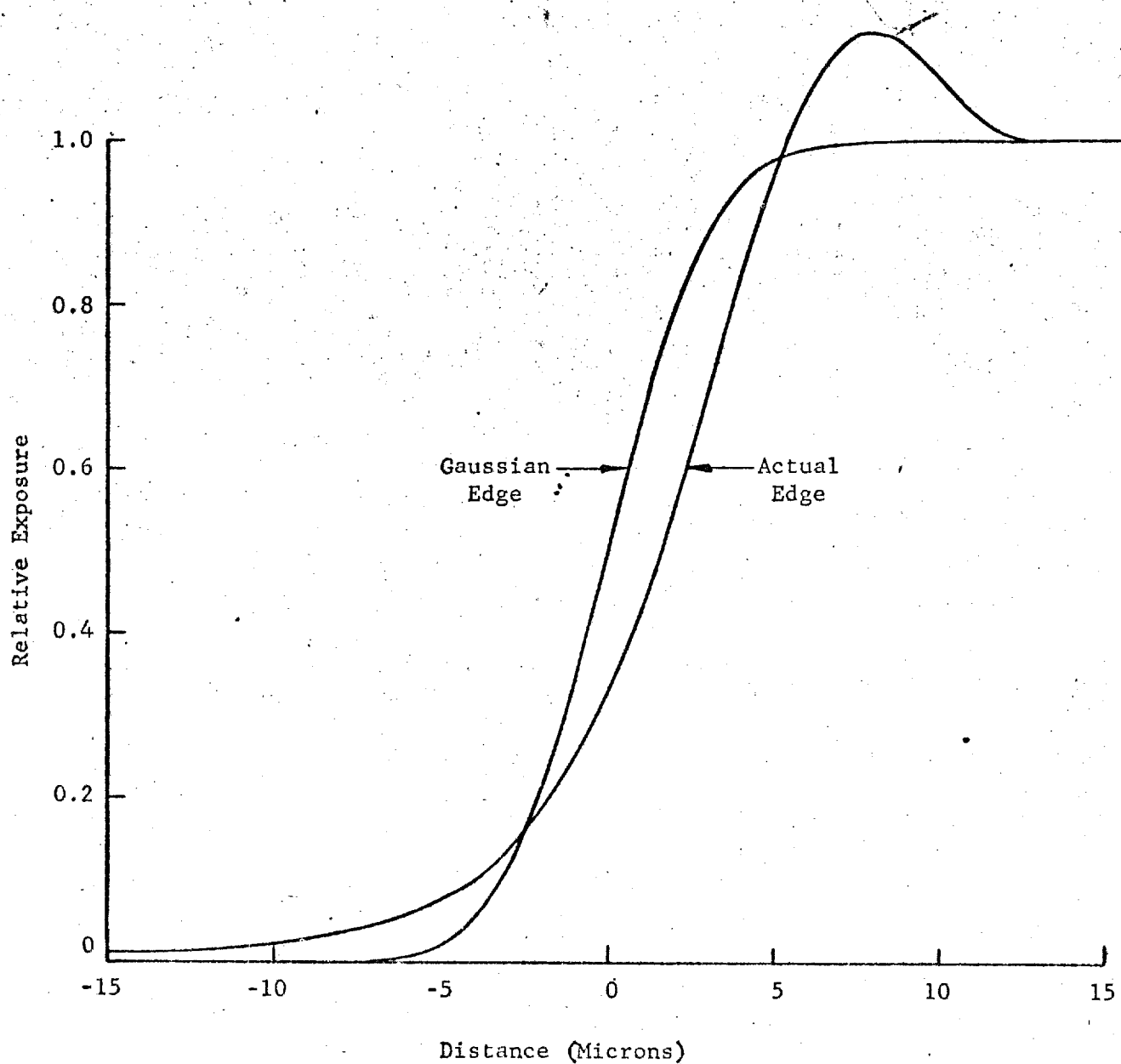


Figure 5. Near-Field Effect
Case D ($K_M = 200$ cy./mm.)

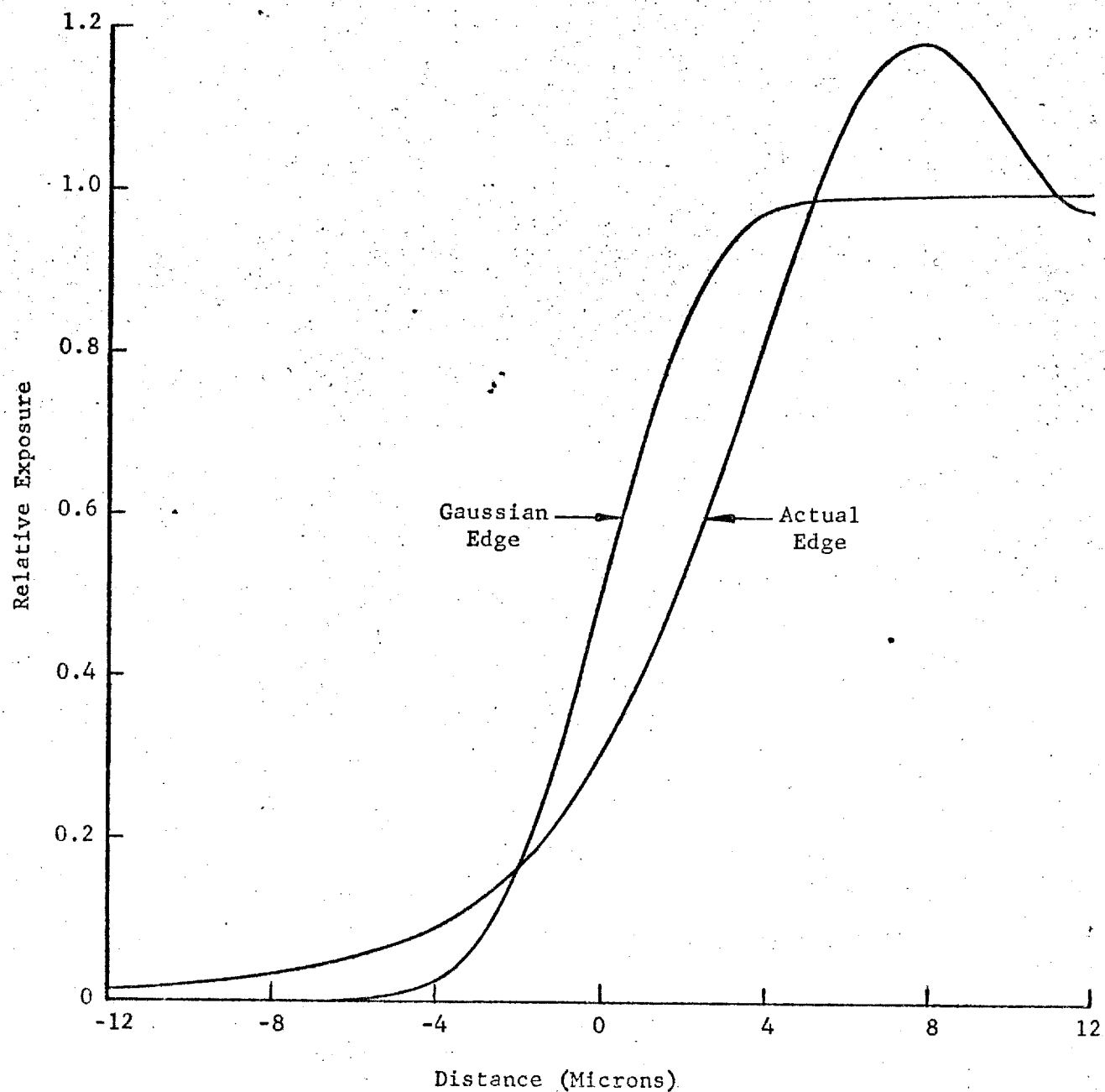


Figure 6. Near-Field Effect
Case E ($K_M = 250$ cy./mm.)

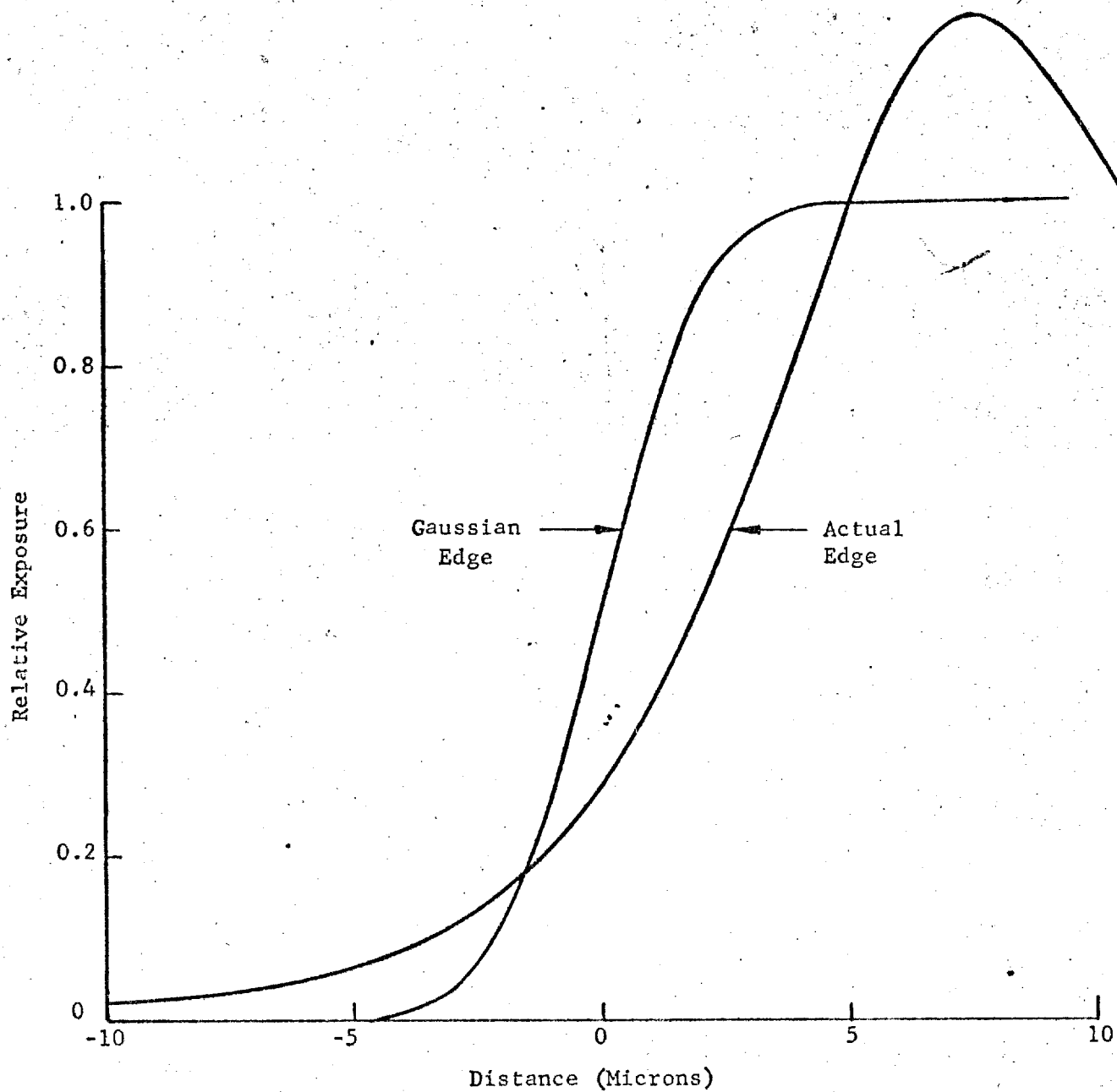


Figure 7. Near-Field Effect
Case F ($K_M = 300$ cy/mm)

By examination of these graphs, several conclusions can be reached. The error for the edge in case A is quite small. This was to be expected since good results had been obtained for the photographic image simulation technique at spatial frequencies of 0 to 100 cycles per millimeter. However, at spatial frequencies of 150 to 300 cycles per millimeter, the edge shape is quite altered by near-field effects. The present simulation procedure evidently cannot produce an exactly specified Gaussian MTF in this spatial frequency range.

It appears that either the present simulation technique must be modified or an alternate procedure must be developed to operate in this higher spatial region.

2.2 PSEUDO GEMS VIEWER MTF CONTROL

The Pseudo GEMS Viewer is to possess the capability of simulating the parameters of MTF, contrast, and exposure when employing a gamma 2.2 negative transparency as a master. The MTF control involves the convolution of a non-linear film image spread function with the degrading linear spread function elements of the viewer optical system. The process of convolving linear and non-linear spread functions is not necessarily predictable or controllable. However, under certain conditions, it is quite possible that the resulting convolution will yield a fair approximation of the desired spread function or transfer function.

An analysis was performed to determine the degree of discrepancy that would result in the MTF simulation by the Pseudo GEMS Viewer approach.

2.2.1 Investigation Procedure

The analytical investigation involved the convolution of a non-linear spread function (designated to represent the film imagery) with a linear Gaussian spread function (designated to represent the viewer optics) for conditions that normally would be encountered in the simulation process. Three Gaussian exposure edges were generated with density ranges of 0.4 to 1.2, 0.8 to 1.6, and 1.2 to 2.0. The relative exposure density ranges of the edges were chosen such that the edges covered the principal exposure range of a typical gamma 2.3 film characteristic curve, Figure 8.

Once the minimum exposure, E_{\min} , and maximum exposure, E_{\max} , values for a particular edge were defined, the exposure versus distance values for the edge, $E(x)$, were generated by integration of a Gaussian spread function.

$$E(x) = E_{\min} + (E_{\max} - E_{\min}) E'(x)$$

where

$$E'(x) = \int_{-\infty}^{x/\sigma} e^{-t^2/2} dt$$

In the above expression, σ is a constant determined from the Gaussian transfer function for the film image:

$$T(k) = e^{-2 (\pi \sigma k)^2}$$

(x is the distance and k is the spatial frequency in the above equations).

By using the procedure described above, the exposure edges for the three density ranges were generated to correspond to a Gaussian transfer function of 160 cycles per millimeter at 0.1 modulation.

In the integration of the spread function, the edge plateaus were defined with 20 points, each; and the gradient was defined with 30 points. The exposure values of these points were determined at a 0.17 micron increment and with a four place decimal accuracy.

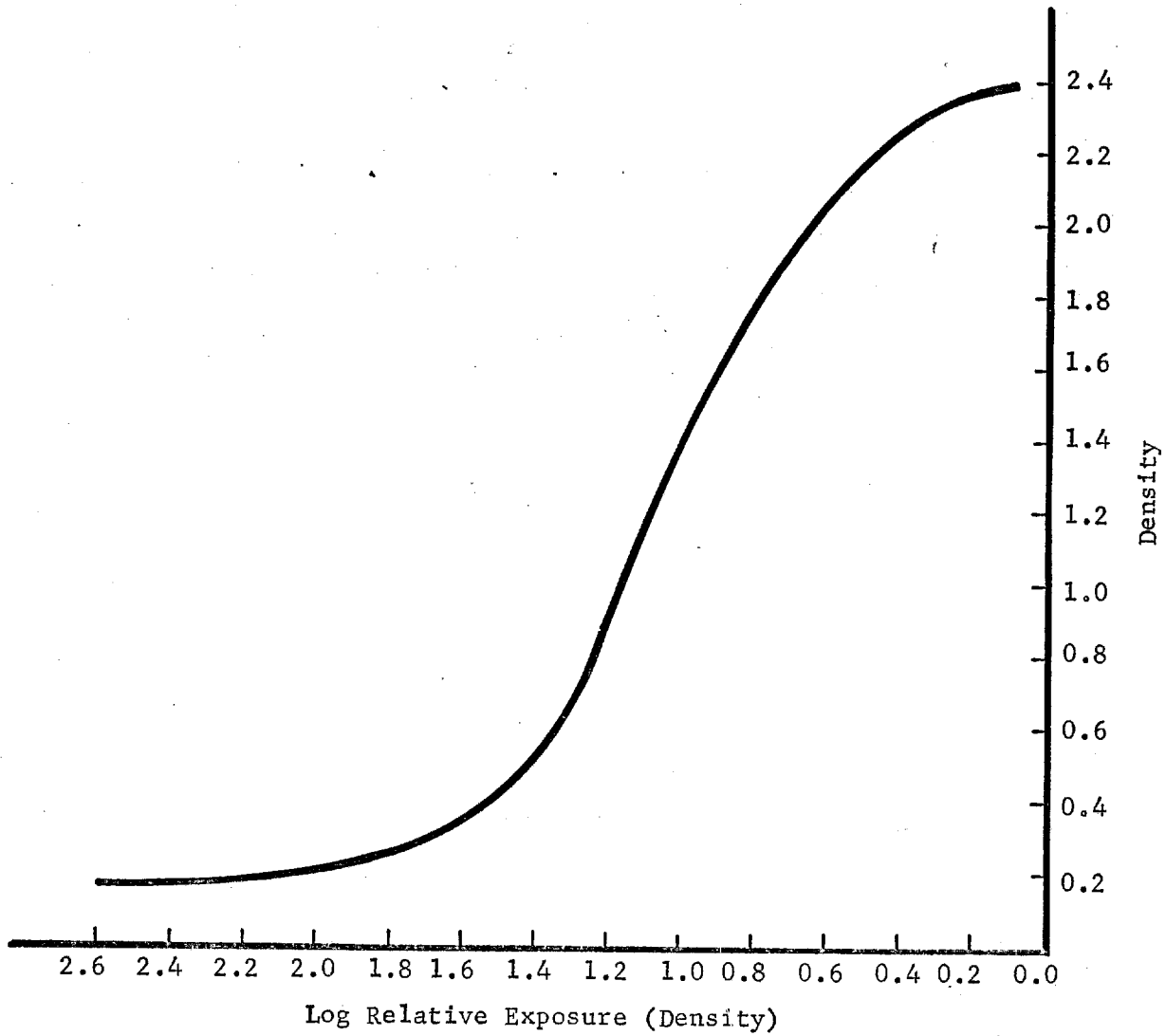


Figure 8. Gamma 2.3 Characteristic Curve

The three exposure edges were converted to film transmittance edges via the gamma 2.3 sensitometric curve. Both the generated Gaussian

STATINTL

exposure edges and the film transmittance edges were processed on the STATINTL

EGA program to obtain transfer functions and modified image transfer functions, respectively. The film transmittance edge gradients were processed on the EGA program without sensitometric data. Therefore, the resulting curves are not transfer functions in the true sense; and, for purposes of discussion in this report, they will be termed modified image transfer functions. The exposure edge gradients were inputted to the EGA program only as a verification of their analytical determination accuracy. The resulting EGA curves are displayed in Figure 9.

It should be noted that each of the film transmittance edge gradients yielded modified image transfer functions with spatial frequency ranges in excess of 160 cycles per millimeter at 0.1 modulation. If imagery were employed in the Pseudo GEMS Viewer, corresponding to the quality of the film edge, and if it was desired to simulate a true MTF, corresponding to 160 cycles per millimeter, the degrading elements of the viewer optics would be constructed so that the product MTF of the optical elements and the modified image transfer function would be 160 cycles per millimeter at 0.1 modulation.

To investigate the simulation of a particular MTF level, each of the three resulting modified image transfer functions was multiplied by a fixed Gaussian MTF curve, representing the viewer optical degrading elements. It should be recalled that the edges are representative of Gaussian MTF curves. In a valid simulation process, where the optics also are described by a Gaussian MTF curve, the product MTF curve of the edge and the optics would normally be a Gaussian. Since the modified image transfer functions are no

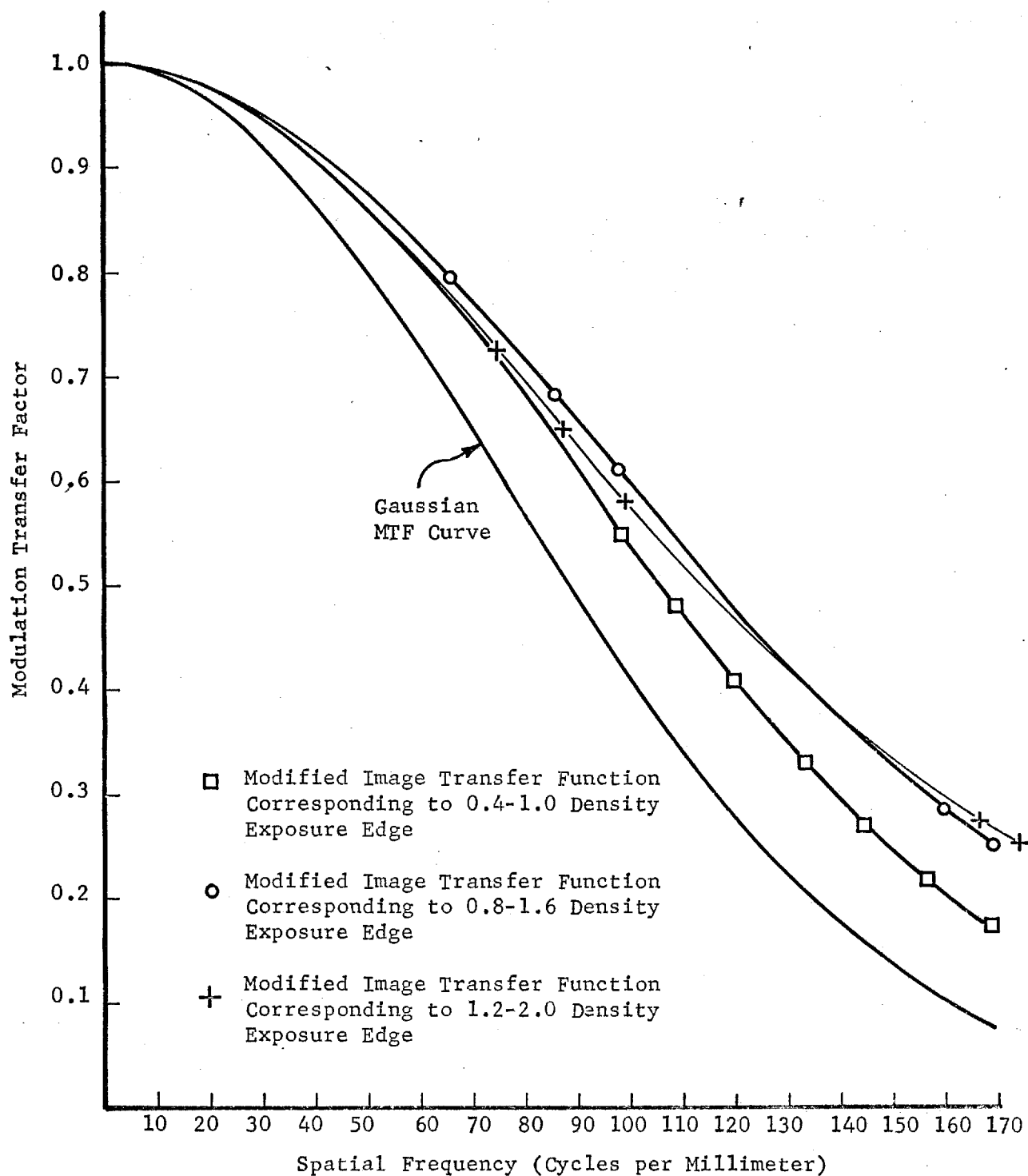


Figure 9. Resulting EGA Curves

longer Gaussian, the purpose of the analysis will be to determine the degree of error introduced by the simulation process for the various regions of the film characteristic curve and for the various levels of MTF simulation. The error analysis will be made with respect to a true Gaussian MTF curve intersecting the 0.1 modulation point at the desired simulated spatial frequency value. The analysis was conducted for the simulated MTF levels of 160, 120, and 80 cycles per millimeter.

To simulate a particular MTF level, the position of the Gaussian MTF curve, representing the optics, was fixed so that the product of the Gaussian MTF and the modified image transfer function, corresponding to the 0.8 to 1.6 density exposure edge, yielded a 0.1 modulation at the spatial frequency value to be simulated. Product MTF curves then were obtained for the other two modified image transfer functions with this fixed Gaussian curve. Each of the three resulting product MTF curves for a particular simulated MTF level was compared to a Gaussian MTF curve that was positioned to intersect the 0.1 modulation point at the desired simulated spatial frequency value. Measures of the simulated MTF errors were obtained for the maximum spatial frequency departures between the product MTF curves and the Gaussian MTF curve.

2.2.2 Results and Conclusions

The comparisons between the simulated transfer functions and the Gaussian transfer functions for the three levels of MTF are displayed in Figures 10 through 12. The graphs show that the greatest MTF disagreement exists in the highest spatial frequency simulation. The spatial frequency error, between the two curves, for all three regions of the characteristic curve at a 160 cycles per millimeter, ranges from 5.5% to 9.5%.

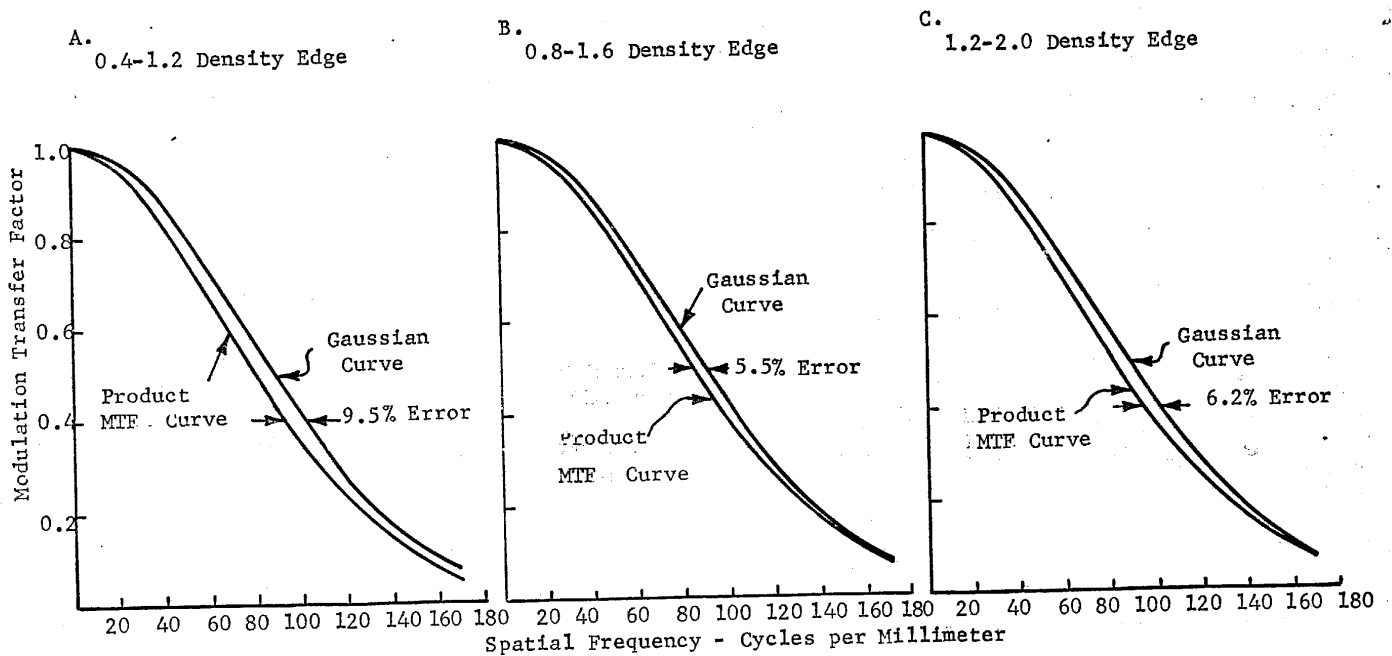


Figure 10. 160 cyc/mm Simulation

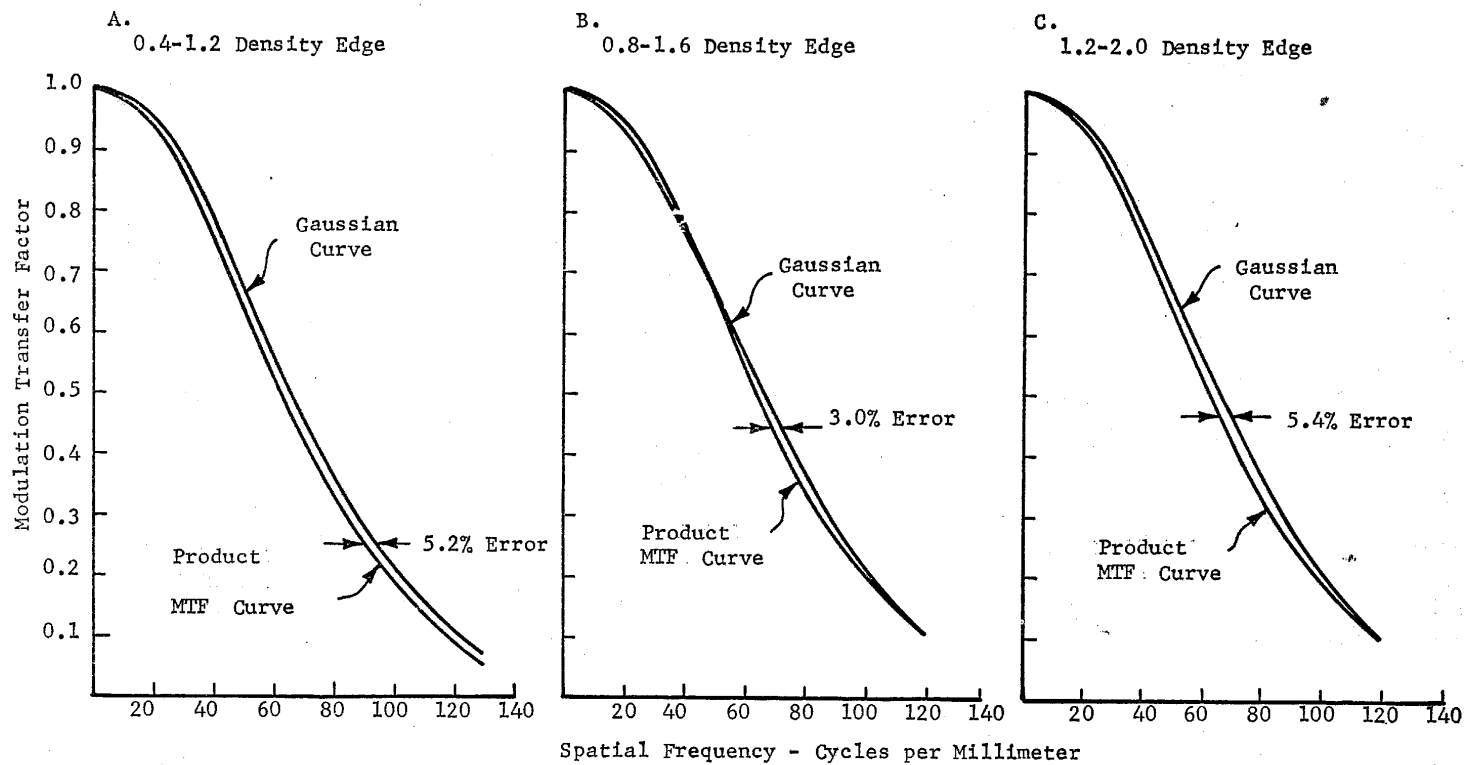


Figure 11. 120 cyc/mm Simulation

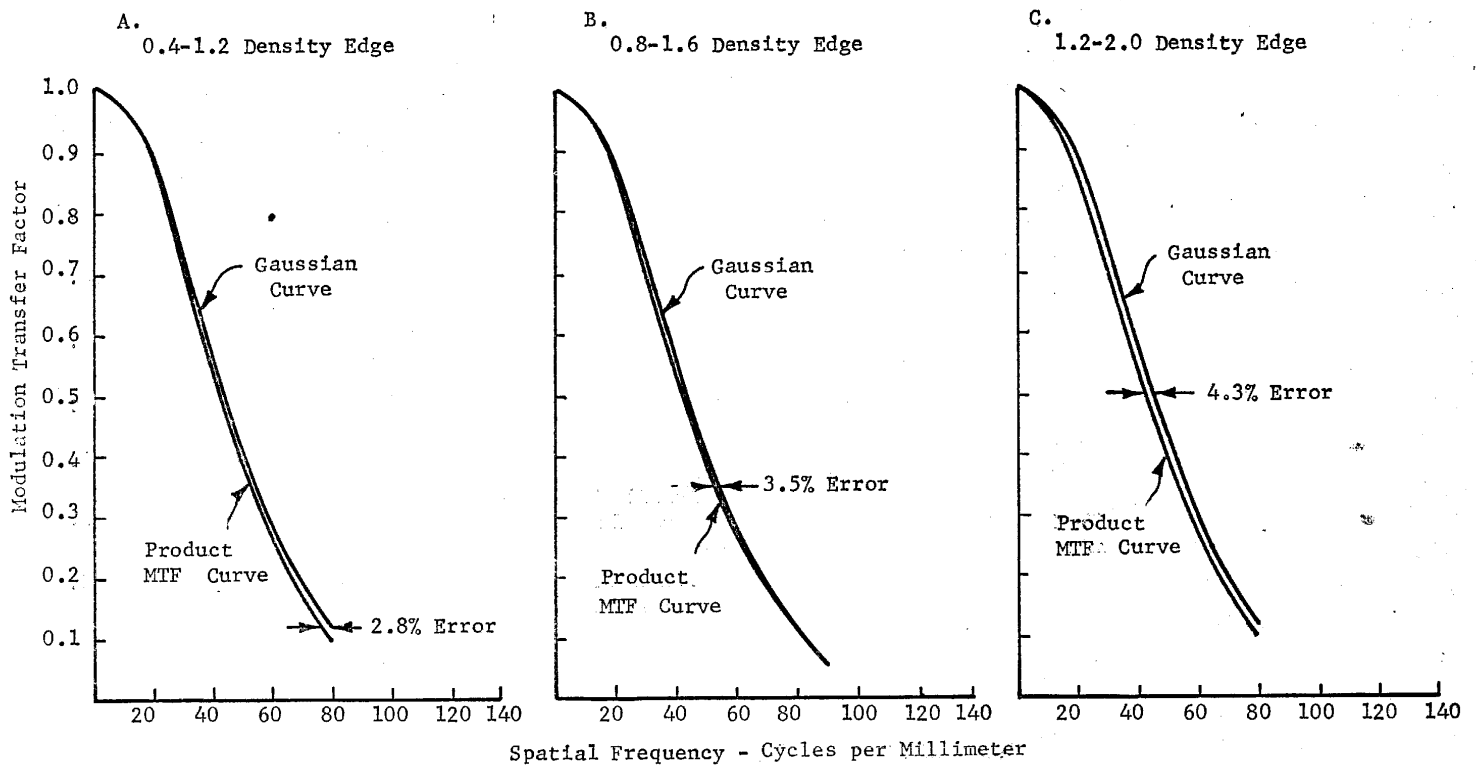


Figure 12. 80 cyc/mm Simulation

It should be noted that the error range for the worst simulated MTF level can be reduced to less than 4% by letting a transfer function other than a Gaussian represent the degrading elements of the viewer optics.

The results of the study clearly indicate that MTF simulation by the Pseudo GEMS Viewer approach can be accomplished for the entire tonal range of the gamma 2.3 imagery and for the spatial frequency extent of 160 cycles per millimeter and below without introducing a significant degree of error.

2.3 EXPOSURE SIMULATION CONTROL

The simulation of exposure involves the duplication of a ground image brightness distribution over the exposure range normally encountered with the camera system. The major factors of concern in the simulation of exposure are the accuracy of GEMS exposure control and the ability to expose the true ground brightness distributions on the GEMS. The latter condition is met by obtaining a positive master transparency whose cascaded film characteristic curve describes a linear relationship between the ground exposure range and the film transmittance range. It has been shown in the Equal Magnification GEMS study that a master transparency with this linear relationship can be achieved.

The accuracy of the GEMS exposure control is a function of the film properties and the GEMS instrument light source. An exposure to the film is related by the expression,

$E = it$, where i is the intensity of the incident light and t is the exposure time. In order to avoid the effect of film Reciprocity Law Failure, which will alter the response characteristics of the film, it is important that the GEMS exposure time be held a constant and that the exposure range be shifted by adjusting the intensity level of the light source. The

light source intensity level adjustment should be accomplished by the addition or the subtraction of neutral density filters over the source. If the intensity adjustment is made by altering the voltage level of the source, a problem with the spectral sensitivity of the source will result.

The accuracy of the GEMS exposure control also is a function of the light source exposure intensity repeatability. In other words, the exposure level among GEMS cannot be held constant unless the intensity of the source is constant for a given exposure time. Experimental tests have indicated that a light source with a $\pm 0.5\%$ variation in its light output energy rating will yield exposure level variation well within the tolerance limits of a densitometer employed to evaluate exposure shifts.

2.4 HAZE SIMULATION CONTROL

A study program was undertaken to determine the accuracy of the haze simulation. Analytical equations describing the resulting hazed image tonal relationships indicate that the basic haze simulation concept is similar to the conditions of photographing a real aerial scene obscured by atmospheric haze. It is true that the effects of back-scatter into shadow areas cannot be simulated; but for diagnostic estimates of the degree of atmospheric haze present in a photograph, this factor is trivial in nature.

The technique of generating GEMS with specific haze modulation values is limited to empirical determination due to the complexity of the photographic process and the lack of appropriate theory to describe the phenomena. With a careful choice of procedures, the empirical approach to simulating haze will not hinder the production aspects of generating material.

2.4.1 Haze Study

The technique of simulating haze consists of printing a positive master transparency onto film which previously was given a uniform fogging exposure. By appropriate sensitometric analysis, the effective film image modulation can be determined. To accomplish the analysis, a sensitometric strip was placed on the unexposed film and given a fogging exposure. A second sensitometric strip was placed on the fogged film and both strips were given what is termed an image exposure.

These strips allow one to find two characteristic curves for the given exposures. By monitoring the maximum and minimum density values of the GEMS transparency, these values can be traced from the reduced contrast curve through the total exposure curve to obtain the effective exposure values for the master transparency density values. Figure 13 shows this procedure where points 1 and 2 are the maximum and minimum exposure values from the master transparency; curve A is the reduced contrast curve; points 3 and 4 are the effective maximum and minimum exposure values as traced from curve A through curve B; and curve B is the total exposure curve.

The technique described resulted in what appeared to be the desired effect, that is the contrast of the print from the master was reduced, but no information exists to define how closely the haze simulation approaches a realistic condition. Another problem is that the effective exposure modulation resulting from a combination of pre-exposure and image exposure is not readily predictable. Therefore, it was decided that a study program would be undertaken to gain insight into the problems of the haze simulation technique so that a well controlled procedure could be employed to generate a realistic simulation of the effects of atmospheric haze upon an aerial photograph.

- 1 & 2 - Maximum & Minimum Actual Exposure, Respectively
3 & 4 - Maximum & Minimum Effective Exposure, Respectively
Curve A - Reduced Contrast Curve
Curve B - Total Exposure Curve

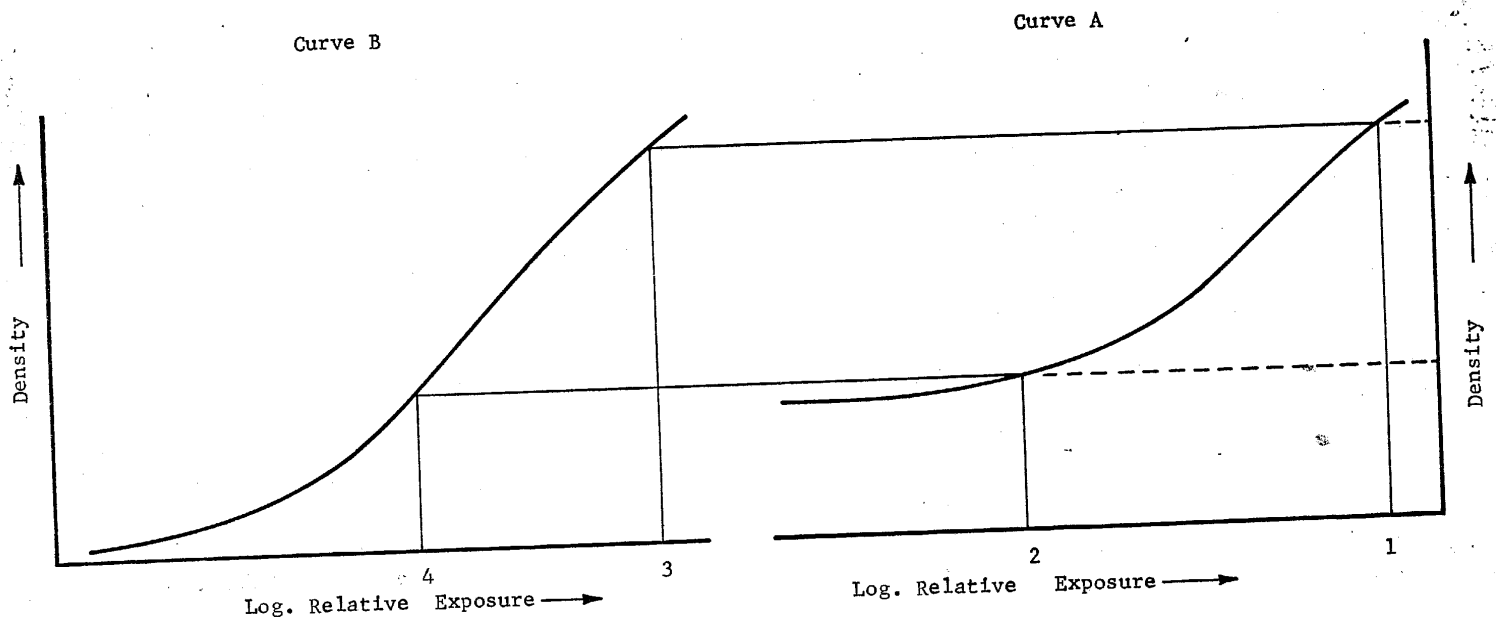


Figure 13. Determination of Effective Exposure

A survey of published literature indicated that the phenomena of atmospheric haze has been extensively researched by others.^{1,2,3} Analytical equations were obtained from the survey which describe the effects of atmospheric haze over the luminance range of an aerial scene. Using tone reproduction analysis, it is relatively easy to compare the characteristics of haze simulated aerial photographs to the results one would have obtained from a real aerial photographic system.

The technique that has been used to simulate exposure modulation reductions due to atmospheric haze consists of printing a master transparency onto photographic film that has been uniformly pre-exposed (fogged). If the two intermittent exposures are additive, their effective exposure should be the same as the exposure the film would have received under real conditions. The basis for this reasoning is founded on the understanding that the effect of atmospheric haze is essentially the addition of uniform non-image forming light to the imaging system. Using the equation for the haze relationship and the equation for calculating the exposure for a camera image, it can be shown that under real conditions of photographing haze obscured scenes, the film receives the same two exposures as the simulated photography, the only difference being that both exposures are produced simultaneously instead of intermittently as in the laboratory situation.

The equation for atmospheric haze is:

$$B_o = B_g + k B_x, \quad (1)$$

where: B_o = luminance of the object on the ground as seen from some altitude,
 B_g = luminance of the ground object corresponding to B_o ,
 B_x = maximum ground scene luminance, and
 k = atmospheric luminance as a fraction of B_x .

The result of adding a constant luminosity to the ground scene luminances is to reduce the luminous contrast of the scene which also reduces the exposure modulation which is defined as:

$$\text{Modulation} = \frac{E_{\max} - E_{\min}}{E_{\max} + E_{\min}}, \quad (2)$$

where: E_{\max} = maximum exposure to the film, and
 E_{\min} = minimum exposure to the film.

The exposure that the film receives can be calculated using the equation for determining the illuminance of any given area in the camera image plane as follows:^{4,5,6}

$$I_o = B_o T \left(\frac{1}{4} f^2\right) (F/V)^2 H \cos^4 \theta, \quad (3)$$

where: I_o = image illuminance,
 B_o = object luminance,
 T = lens transmittance,
 f = lens f number,
 F = focal length of lens,
 V = image distance,
 H = vignetting factor of lens barrel, and
 θ = angle of image off lens axis.

The above equation gives the image plane illuminance for any object. But, for objects on axis and at a large distance from the camera, equation (3) becomes:

$$I_o = B_o T / (4f^2), \quad (4)$$

when $H = 1.00$.

Camera lens flare may be considered separately in this equation; but for most lenses in use today, the amount of flare is small relative to the effect of haze. Therefore, the flare may be included in the equation for haze. Equation (1) may be substituted into equation (4) to give:

$$I_o = (B_o + k B_x) T / (4 f^2) \quad (5)$$

If the exposure time is now accounted for:

$$E = I_o t = t (B_o + k B_x) T / (4 f^2) , \quad (6)$$

where t is the exposure time.

It can be shown that equation (6) represents two separate exposures; the first for the camera image and the second for the haze. Equation (6) then may be written as:

$$E = E_1 + E_2 = \frac{t B_o T}{4 f^2} + \frac{t k B_x T}{4 f^2} , \quad (7)$$

where $\frac{t B_o T}{4 f^2}$ is the image exposure, and

$\frac{t k B_x T}{4 f^2}$ is the exposure due to haze.

It is evident from these equations that the technique used to simulate the exposure modulation reduction due to atmospheric haze will produce a replication of haze as long as there is no effect due to the separate and intermittent exposures given to the simulated photograph.

Having found the basic technique for producing exposure modulation reductions to be sound, the equations used in the modulation reduction prediction process were examined. Equations were derived to permit the calculation of exposures values for reducing the exposure modulation of a master transparency.^{7.8}

The first of these equations is used to calculate the ratio of the pre-exposure to the image exposure:

$$R = \bar{T} \frac{M_T}{M_S} - 1, \quad (8)$$

where: M_T = transmission modulation of the transparency to be printed,

M_S = desired print exposure modulation,

\bar{T} = average transmission of the transparency,

$R = I_1 / I_2$, t_1 / t_2 , or T_f / T_{ND} .

The terms given for R are defined as:

I_1 - intensity of pre-exposure illumination,

I_2 - intensity of image-exposure illumination,

t_1 - pre-exposure time,

t_2 - image exposure time,

T_f - transmittance of neutral density filter used to modulate pre-exposure illumination, and

T_{ND} - transmittance of neutral density filter used to modulate image exposure illumination.

Three ratios are given for R , and the one used will depend upon the variable chosen to control the exposure to the film. The exposure is related by the equation:

$$E = ItT, \quad (9)$$

where: E = exposure to the film,

I = intensity of illumination,

t = time, and

T = transmission of printing system.

If two of the three independent variables are held constant, the exposure will be controlled by the third variable. This point may be illustrated by discussing the printing system used to generate the simulated photographic material. In this case, the exposure time and illumination are held constant, and the exposure is controlled by introducing filters varying the transmission of the printing system.

The transmission modulation, M_T , in equation (8) is identical to the maximum exposure modulation for the simulated photograph being printed. The effective exposure modulation desired is M_S , and M_S must always be equal to or less than M_T .

$$M_S \leq M_T$$

Having specified M_S and determining how the exposure will be controlled, a second equation is used to calculate the specific pre-exposure and image exposure conditions. The variable of this equation is dependent upon the selection of constants from equation (8):

$$T_{ND} = \frac{10^{\frac{\gamma^8}{D}}}{It \sqrt{(T_X T_N) + (T_X + T_N)R + R^2}} \quad (11)$$

where: O_D is the opacity of the print average density value,

γ is the gamma of the print,

I is the intensity of exposing light source,

t is the exposure time,

T_X is the maximum transmission of the master transparency,

T_N is the minimum transmission of the master transparency, and

i is the speed index of the print film.

The ratio of I/i can be computed from equation (11) by letting R equal zero; this is the case for making a print with no exposure modulation reduction. This computation is necessary since i and I are not known for the system presently employed. All other values may be measured. The reciprocal of I/i may now be substituted back into equation (11), and the equation used for calculating a new T_{ND} where R is a value calculated from equation (8). The resulting T_{ND} value from equation (11) then is used to solve the last unknown, T_f , using the equation:

$$T_f = T_{ND} R. \quad (12)$$

In the preceding paragraphs an analytical analysis of the haze theory was presented, and the technique for simulating haze by an exposure modulation reduction of an aerial photograph was developed. However, in applying the theory the simulation of back-scatter cannot be accomplished. Although equation (1) accurately describes the effect of atmospheric haze, it does not account for the effect of back-scatter in shadow areas. Where in real life, there exists a significant degree of back-scatter, shadow areas in a scene are illuminated so that details in these shadow areas become detectable. If shadow detail is not present in the master transparency, it cannot be recorded in the simulation process. It should be noted that valid estimates of exposure modulation reduction are not dependent upon the faithful simulation of shadow detail. Therefore, this simulation deficiency is of little significance.

2.4.2 Haze Experimentation

The analytical equations were used to predict experimental exposure modulation reduction values. An experimental effort was conducted in the laboratory to determine the accuracy of the simulations based upon these predictions.

Table 2 is a summary chart of the experimental results. In most cases, the error that exists between the measured and the predicted values is less than 10 percent. The results indicate that the theoretical equations failed to provide valid predictions and that these equations only serve to furnish estimates of the required exposure values. By empirical determination the error can be constrained to a quite tolerable 3 percent level. However, upon examination of the resulting haze sensitometric curve shapes, Figure 14, it can be seen that the exposure modulation reduction corresponding to the maximum scene modulation, is correct; but that the intermediate scene modulations are in error.

Figure 14 is an example of a typical haze simulation generated in the laboratory where the maximum and minimum scene density values have been altered to yield the desired exposure modulation reduction. In diagram (1), the theoretical haze curve to be simulated is labeled as curve A. Diagram (2) represents the characteristic curve for the film-developer combination and for the total exposure of the simulation process. Curve C of Diagram (3) is the resulting simulated haze sensitometric curve, and curve D is the theoretically predicted haze sensitometric curve. The differences that exist between curves C and D give an indication of the haze simulation error for the full image tonal scale. If curve C is transposed through the tone reproduction cycle to Diagram (1), the simulated haze curve, curve E, would be obtained.

The error represented by the haze sensitometric curves, curves C and D, is a result of such reciprocity effects as latensification, and hypersensitization, intermittancy effect, and low intensity desensitization. These effects are present because of the double exposure steps of the simulation process. It is quite obvious that the low contrast imagery in the vicinity of

TABLE 2

Predicted vs. Measured Exposure Modulation Values

Predicted Exposure Modulation	Measured Exposure Modulation	Percent Difference	Average Density of Simulated Photograph
0.88	0.88	0.0	1.34
0.70	0.84	20.0	1.46
0.60	0.64	6.7	1.31
0.50	0.53	6.0	1.32
0.40	0.36	10.0	1.29
0.30	0.31	3.3	1.28
0.20	0.17	15.0	1.29

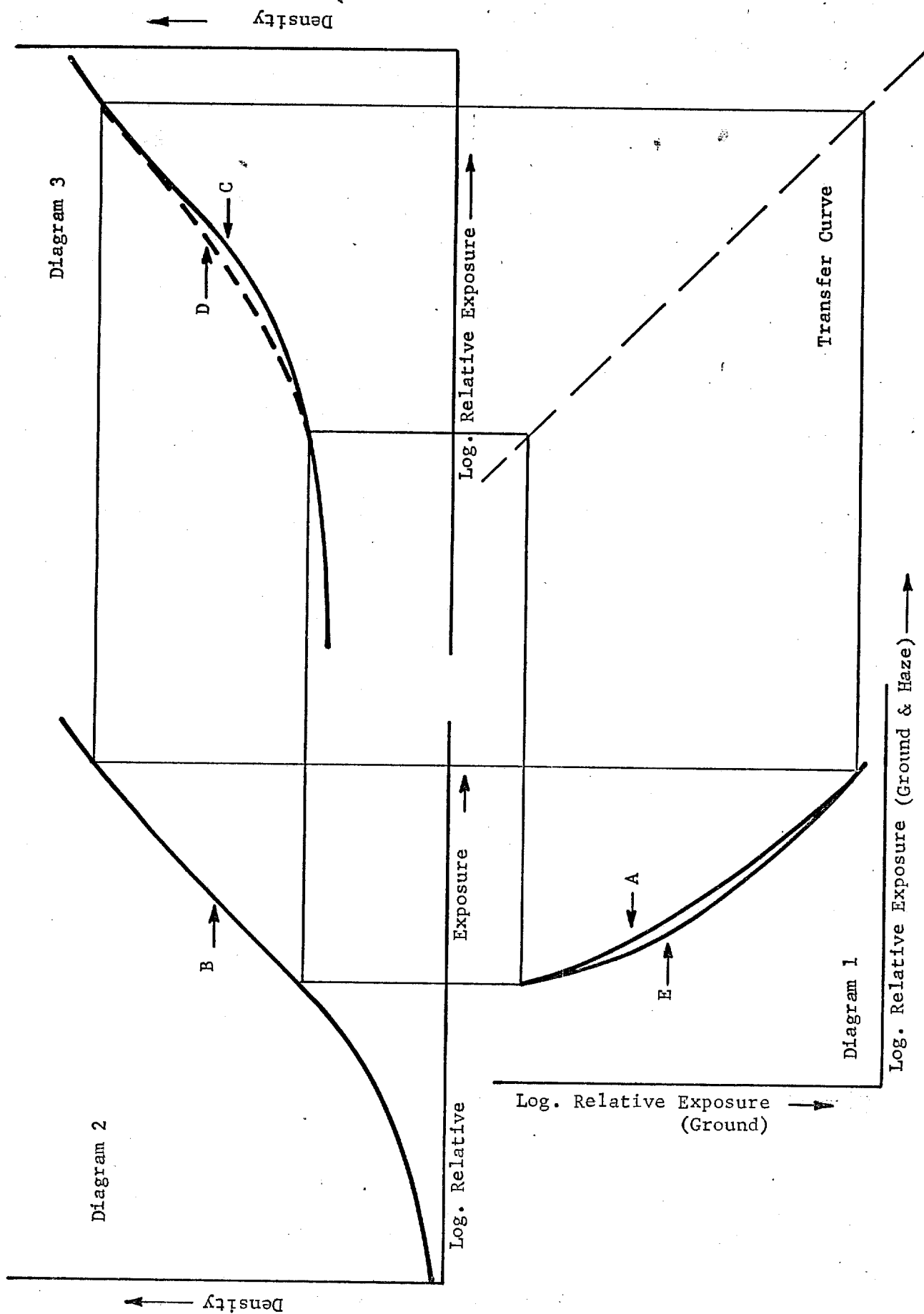


Figure 14. Tone Reproduction Analysis of Atmospheric Haze

the average scene density suffers the greatest simulation error. However, by simulating the best fit sensitometric haze curve, instead of basing the simulation control on the scene maximum and minimum density values, the error associated with the simulation process can be reduced, in most situations, to less than 5 percent for the full image tonal range.

2.4.3 Haze Study Conclusions

The haze study was concerned with defining the physical characteristics of haze, developing an analytical means for predicting and controlling haze in the simulation process, and obtaining a measure of the accuracy of the simulation process. In simplified terms, the physics of a hazed aerial scene is actually the reduction of the scene imagery signal level by a superimposed non-image forming d.c. light level. In reality, imagery which exists in shadow areas is illuminated by what is termed back-scatter. However, the phenomena of back-scatter is not an essential haze simulation feature because, in the evaluation of photography with GEMS, estimates of haze are obtained from the overall visual impression of a scene area and not specific shadow detail.

A means for predicting haze was developed from the theoretical equations that describe the physical nature of haze and the physical characteristics of the film. An experimental effort was conducted in the laboratory to evaluate the prediction process. As a result of the double exposure film effects, the actual and simulated haze curves cannot be identically matched in shape. Basing the predictions on the scene maximum and minimum density values results in simulation errors as great as 20 percent. By making slight image exposure adjustments, a best fit can be obtained between the theoretical haze sensitometric curve and the simulated sensitometric curve. Control of the simulation process in this manner will reduce the simulation error below 5 percent for most simulated haze levels.

The simulation error can be reduced to the error of evaluation by altering the modified contact printer with a d.c. optical illumination system and a beam splitter. Such an alteration would be a minor modification to the existing printer. By employing a d.c. illuminator with a beam splitter, the simulation could be accomplished with one exposure, and the film effects would be eliminated.

2.5 EQUIPMENT MODIFICATIONS AND IMPROVEMENTS

Several instrument modifications were made to the GEMS printer. The base plate of the instrument was replaced with a film vacuum platen and jigging for accurate control of the unexposed film-master transparency separation. The jigging was designed to allow the establishment of printer separations to within ± 0.0002 inches. In considering the simulation of 50 cycle per millimeter material, the need for this degree of control becomes obvious. By substituting into the equation, $r = (R/D) d$, typical parameters for a 50 cycle per millimeter simulation, it can be shown that a variation in "d" of ± 0.0002 inches results in a MTF simulation error of approximately ± 1.5 percent. All other variables in the MTF prediction process, except for the MTFs of the master transparency and the GEMS film, can be determined accurately enough to permit MTF control to within ± 2 percent.

A new light source was installed in the GEMS instrument. The output energy of the 1/1000 second strobe flash unit is regulated to ± 0.5 percent. Regulation of the output energy to this degree of accuracy is required in order to generate small exposure shifts in a GEMS matrix. With a ± 20 percent regulated unit, a 0.06 density exposure shift could not be controlled. Sensitometric evaluation of the new strobe unit demonstrated exposure control of ± 0.01 density units; this density variation is the tolerance of the densitometer

used in the evaluation. It quite likely could be that the variability of the flash unit is much smaller than can be detected by a densitometer.

In generating photographic reductions, a problem with sensitometric control was encountered due to the lens format fall-off characteristics. To obtain valid sensitometric data, it was essential to measure the values of the object plane sensitometric exposure steps in the image plane of the lens. An aerial image read-out device was breadboarded for this purpose. The device consisted of a power supply connected to an RCA 6199 multiplier phototube. A 0.5 millimeter aperture was placed over the tube for the purpose of limiting the size of the step area to be measured. Since the illumination level at the image plane is quite low, the output signal of the tube was amplified. Voltage readings of the exposure steps were obtained with a digital voltmeter.

The device was calibrated for a specific optical setup before using it. The calibration procedure consisted of obtaining voltage measurements from known density steps on the optical axis. To use the device, the density value of a step located off-axis was simply adjusted until the correct calibrated voltage reading, corresponding to the desired step density, was obtained. The device worked quite well. A density change of less than ± 0.01 units could be measured over the low density region, and a density change of ± 0.02 units could be measured at a density of 3.0.

SECTION III

STUDY TASK CONCLUSIONS

3.1 SIMULATION SUMMARY CONCLUSIONS

An analytical investigation was performed to determine the effects of near-field diffraction on the control of MTF when MTF was simulated with the GEMS modified contact printer. The results of the investigation indicated that the simulation of MTF can be suitably controlled below 100 cycles per millimeter. Above 100 cycles per millimeter the Fresnel diffraction effect introduces a sizeable alteration in the shape of an edge. The edge shape alterations are too extensive to allow MTF predictability and controllability in the high spatial frequency regions.

In the simulation of MTF with the Pseudo GEMS Viewer, the non-linear film imagery must be convolved with the degrading linear spread function elements of the viewer optics. An analytical investigation was performed in this area of MTF simulation to determine the error that would result in the MTF control. The investigation demonstrated that a 160 cycle per millimeter MTF simulation could be achieved with less than a 4 percent error for the full tonal range of the imagery. Errors of less than 2 percent would be introduced in an 80 cycle per millimeter MTF simulation. Percentage errors of this magnitude are quite tolerable.

Modification of the GEMS instrument with a well regulated light source has yielded exposure simulations within the tolerance limits of the evaluation equipment. A 0.02 density exposure shift can be simulated.

An analytical and experimental investigation was initiated to determine the accuracy of the haze simulation process. Due to the film effects

created by the double exposure process, haze simulations cannot be achieved with less than a 5 percent error by the present technique. By modifying the GEMS instrumentation with a non-imaging light source, both the fogging exposure and the image exposure can be accomplished, simultaneously; and the film effects would be eliminated. Simulating haze in this fashion is identical to a real haze situation except for shadow areas. The error of the simulation process then would be reduced to the error of the evaluation equipment. It is important to note that to obtain an estimate of haze is not dependent upon the phenomena of shadow area back-scatter.

3.2 INSTRUMENTATION SUMMARY CONCLUSIONS

The GEMS instrument was modified with a film vacuum platen and a strobe flash unit. The vacuum platen and its associated jiggling permit control of the master transparency-GEMS film separation to ± 0.0002 inches. At a MTF simulation level of 50 cycles per millimeter, the instrumentation variables for the modified contact printer can be controlled to ± 2 percent of the desired transfer function. At 100 cycles per millimeter the error increases to slightly less than 4 percent.

A strobe flash unit was installed to improve exposure repeatability and to eliminate the film Reciprocity Law Failure problems introduced by long exposure times. With the new source, an exposure repeatability of ± 0.01 density units is achievable. A ± 0.01 density variability is equivalent to the error of the densitometer used in the exposure evaluation process. It is quite possible that the source has less variability than can be detected with the evaluation equipment.

An aerial image read-out device was breadboarded in order to obtain more accurate measures of sensitometric data in a copy camera reduction system. In a copy system an error is introduced in the sensitometric data if the lens

fall-off properties are not taken into account. To obtain valid sensitometric data, sensitometric step readings must be obtained in the lens image plane. The breadboard device provided sensitometric data within ± 0.01 density units for the low density region and within ± 0.02 density units for the high density region.

REFERENCES

1. Carman, P.D., J. Opt. Soc. Am., 41, 5, 1951.
 2. Manual of Photogrammetry, 2nd Ed., American Soc. of Photogrammetry, Washington, D. C., 1952.
 3. Tupper and Nelson, Photo. Eng., 6:2, 1955
 4. James and Higgins, Fundamentals of Photographic Theory, Morgan & Morgan, New York, 1960.
 5. Jenkins and White, Fundamentals of Optics, Third Ed., McGraw Hill, New York, 1957.
 6. Mees, The Theory of The Photographic Process, Revised Ed., Macmillan, New York, 1959.
-

STATINTL

STATINTL

Approved For Release 2002/06/17 : CIA-RDP78B04747A000700010024-8

Approved For Release 2002/06/17 : CIA-RDP78B04747A000700010024-8